# Stability of nuclei in peripheral collisions in the JAERI quantum molecular dynamics model

Davide Mancusi*
*Nuclear Engineering, Applied Physics, Chalmers University of Technology, Gothenburg, Sweden*

Koji Niita
*Research Organization for Information Science and Technology, Tokai-mura, Japan*

Tomoyuki Maruyama
*College of Bioresource, Nihon Unniversity, Fujisawa, Japan*

Lembit Sihver
*Nuclear Engineering, Applied Physics, Chalmers University of Technology, Gothenburg, Sweden and Department of Mathematics, Computer Science and Physics, Roanoke College, Salem, Virginia, USA*
(Received 22 January 2008; revised manuscript received 20 November 2008; published 29 January 2009)

The JAERI quantum molecular dynamics (JQMD) model has been successfully used for a long time now to describe many different aspects of nuclear reactions in a unified way. In some cases, however, the JQMD model cannot produce consistent results: First, it lacks a fully relativistically covariant approach to the problem of molecular dynamics; second, the quantum-mechanical ground state of nuclei cannot be faithfully reproduced in a semiclassical framework. Therefore, we introduce R-JQMD, an improved version of JQMD that also features a new ground-state initialization algorithm for nuclei. We compare the structure of the two codes and discuss whether R-JQMD can be adjusted to improve JQMD's agreement with measured heavy-ion fragmentation cross sections.

DOI: 10.1103/PhysRevC.79.014614 PACS number(s): 24.10.Lx, 24.10.Jv, 25.75.−q, 25.70.Mn

## I. INTRODUCTION

The relevance of intermediate-energy heavy-ion reactions (between a few hundred and a few thousand $A$ MeV) for radiation-transport problems has always motivated, at least partly, the study of such processes. Besides the exciting theoretical puzzles (such as the determination of the parameters of the nuclear equation of state [1,2], the nature of the multifragmentation phenomenon [3,4], and the flow of nuclear matter [1]) that have driven research since intermediate-energy heavy-ion beams became available, applications in other fields of physics, such as the propagation of the galactic cosmic rays (GCRs) [5], have always motivated the development of reliable models.

More recently, the advent of the *International Space Station* and the prospect of long-term manned interplanetary missions have introduced yet another challenging context for the problem of the transport of energetic cosmic rays in matter and, more specifically, for the improvement of nuclear-reaction models. Heavy ions in GCRs are in fact responsible for the delivery of a considerable share of the radiation dose outside the protective influence of Earth's atmosphere and magnetic field, in spite of their relatively low abundance [6]. Presently, the only feasible countermeasure to GCR exposure is represented by shielding, which can soften the composition of the radiation field and reduce exposure risks; however, quantitative risk estimates must rely on the detailed knowledge of the radiation spectra inside the spacecraft, which requires the employment of an accurate nuclear-reaction model.

The JAERI quantum molecular dynamics (JQMD) model [7] was developed in the beginning of the 1990s with the intent to provide a unified description of various aspects of nuclear reactions; it belongs to the family of quantum molecular dynamics (QMD) models [2]. By feeding the output of JQMD to a statistical decay code such as the statistical decay model (SDM) [7] or the generalized evaporation model (GEM) [8], one obtains a hybrid model that can describe accurately both the fast dynamical stage and the slow statistical stage of the reaction and, thus, can reproduce measured double-differential cross sections for the production of protons and neutrons in proton-nucleus and nucleus-nucleus collisions [7].

There are other observables, however, that JQMD does not reproduce as accurately as double-differential cross sections for nucleon production; for example, fragment yields in heavy-ion reactions are sometimes in sensible discrepancy with the experimental data [9], especially for soft, peripheral reactions that only entail stripping of a small number of nucleons. The cause of these shortcomings can be traced back to a small intrinsic instability of the ground state of the JQMD nucleus, which in fact can emit nucleons spontaneously because of potential-energy fluctuations and alter significantly the final yields of soft, peripheral reactions (since hard, central collisions are not very sensitive to the details of the initial configuration).

These instabilities arise for two main reasons: First, the JQMD formalism is not completely relativistically covariant, which implies that the dynamics of a nucleus is somehow dependent on the frame of reference used. Second, the

*d.mancusi@ulg.ac.be; Presently at Fundamental Interactions in Physics and Astrophysics, University of Liège, Liège, Belgium.

 

ground state in which JQMD nuclei are initialized is only an approximation; in all QMD models, it is conceptually impossible to create the "real" ground state, that is, the lowest-energy eigenstate of the quantum-mechanical $n$-body Hamiltonian operator, which is influenced by Pauli's exclusion principle. (In a semiclassical $n$-body theory, such as QMD models, Pauli's principle is not taken into account and particles are thus allowed to move closer to each other.) Thus, if we want to describe peripheral nucleus-nucleus reactions consistently in the JQMD framework, it is necessary to switch to a relativistically covariant formalism and to improve the ground-state initialization algorithm, to suppress spurious potential-energy fluctuations and particle decays.

This paper describes R-JQMD, a new version of the JQMD model that includes a covariant treatment of two-body interaction and scattering and that incorporates an improved ground-state initialization algorithm. Other relativistic QMD models have already been described [10,11]. Section II will summarize briefly the structure of the JQMD model and point out some of its limitations; Sec. III describes the R-JQMD model; Sec. IV presents some results of calculations with R-JQMD; in Sec. V we discuss the possibility of improving the accuracy of heavy-ion fragmentation cross sections by tuning the impact-parameter distribution; finally, in Sec. VI, we draw some conclusions.

## II. STRUCTURE AND LIMITATIONS OF THE JQMD CODE

Let us summarize here briefly the main assumptions of the JQMD model.

### A. Generic assumptions

Nucleons are assumed to be described by coherent states of fixed width:

$$\varphi_i(\boldsymbol{r}) \equiv \frac{1}{(2\pi L)^{3/4}} \exp\left(-\frac{(\boldsymbol{r}-\boldsymbol{r}_i)^2}{4L} + \frac{\imath}{\hbar}\boldsymbol{r}\cdot\boldsymbol{p}_i\right), \tag{1}$$

where $\boldsymbol{r}_i$ and $\boldsymbol{p}_i$ are the centroids of the configuration-space and momentum-space distributions of the $i$th nucleon. The total wave function is taken to be the direct product of the single-particle wave functions,

$$\psi(\boldsymbol{r}_1, \boldsymbol{r}_2, \ldots, \boldsymbol{r}_N) \equiv \prod_i \varphi_i(\boldsymbol{r}_i), \tag{2}$$

which is equivalent to assuming that the particles are distinguishable. Of course, nucleons are actually indistinguishable, but it is assumed that their fermionic nature can be mimicked by a suitable choice of the two-body potential.

### B. Dynamics

The dynamical evolution of the system alternates a transport step and a collision step. In the transport step, each particle moves (semiclassically) under the influence of the two-body potentials generated by all the other particles; in the collision step, particles scatter on each other and/or decay, producing new particles or resonances.

#### 1. Equations of motion

All the transport is described by the phase-space trajectories $[\boldsymbol{r}_i(t), \boldsymbol{p}_i(t)]$ of the particles; the equations of motion for the evolution of these trajectories are derived from a generalized Ritz variational principle, since a wave function of the form of Eq. (2) (e.g., with fixed packet widths) cannot solve Schrödinger's equation exactly. If a Hamiltonian operator of the form

$$\hat{H} \equiv \sum_i \left(\sqrt{\hat{\boldsymbol{p}}_i^2 + {m_i}^2}\right) + \hat{V} \tag{3}$$

is assumed, the equations of motion for the centroids $\boldsymbol{r}_i$ and $\boldsymbol{p}_i$ have the form of Hamilton's equations and read

$$\dot{\boldsymbol{r}}_i = \frac{\boldsymbol{p}_i}{m} + \frac{\partial\langle\hat{V}\rangle}{\partial\,\boldsymbol{p}_i}, \tag{4a}$$

$$\dot{\boldsymbol{p}}_i = -\frac{\partial\langle\hat{V}\rangle}{\partial\boldsymbol{r}_i}. \tag{4b}$$

The effective potential $\hat{V}$ is assumed to include a Skyrme-type interaction, a Coulomb interaction, and a symmetry term. Since all these two-body interactions depend on the distance $\boldsymbol{r}_{ij}$ between the centroids of the particles $i$ and $j$ in configuration space, which is not a Lorentz scalar, the potential will not be a Lorentz scalar, either. Relativistic covariance is partially restored by substituting $\boldsymbol{r}_{ij}^2$ with a Lorentz scalar such as

$$\tilde{\boldsymbol{r}}_{ij}^2 \equiv -{q_{ij}}^2 + \frac{(q_{ij}\cdot p_{ij})^2}{{p_{ij}}^2}, \tag{5}$$

where $q_{ij} \equiv q_i - q_j$ is the four-dimensional distance and $p_{ij} \equiv p_i + p_j$ is the total four-momentum. The scalar $\tilde{\boldsymbol{r}}_{ij}^2$ reduces to the square of the normal distance in the center-of-mass frame of particles $i$ and $j$, which is acceptable because this is the only frame where the two particles are treated on the same footing. The substitution, however, makes the effective potential momentum dependent.

#### 2. Two-body collisions

Stochastic collisions are introduced phenomenologically, similarly to the BUU/VUU approach, respecting energy and momentum conservation. Particles are assumed to collide if their (covariantly defined) impact parameter is smaller than a given value determined by their cross section. Presently, JQMD includes production of $\Delta(1232)$ and $N^*(1440)$ resonances and their decays into baryons and pions. Since no essential modifications have been made to the collision step in the R-JQMD code, we refer the reader to Ref. [7] for more details about how cross sections are parametrized in JQMD.

### C. Initialization

Before the dynamics of a heavy-ion reaction can be simulated, it is necessary to initialize the nuclei in a suitable state. In nature, the two colliding nuclei are usually in their ground states; however, as we have anticipated in Sec. I, there is an intrinsic, conceptual difficulty in the definition of ground state in a semiclassical model such as JQMD. The

lowest energy state in JQMD is more tightly bound than the quantum-mechanical ground state, because the kinetic energy of the nucleons can be reduced without violating Pauli's principle (which does not apply to JQMD). Thus, the state in which JQMD nuclei are actually initialized is not the lowest energy state of the model, but rather an adjusted configuration that is optimized to approximate some characteristics of the quantum-mechanical ground state.

In particular, particle positions are drawn randomly from a Woods-Saxon-type distribution, whereas momenta are uniformly sampled in a sphere of radius equal to the local Fermi momentum; the single-nucleon wave packet width is ignored at this stage—it influences the dynamics only through the equations of motion. A minimum distance is imposed between particle positions, to reduce density fluctuations. The state so obtained is rejected if any of the particles has a positive total energy or if the Pauli principle is violated; this condition is checked by calculating the phase-space overlap of each nucleon with all the others [12].

If the state created has been accepted, its binding energy is adjusted to reproduce the value provided by a simple liquid-drop formula [13] by "heating up" or "cooling down" the nucleus: One lets the nucleons evolve according to their equations of motion (as described in Sec. II B 1) with the addition of a (positive or negative) frictional term, which provides or subtracts the necessary amount of energy over a few time steps.

Once the optimal ground-state energy is attained, the nucleus is Lorentz-boosted to the center-of-mass frame of the reaction.

### D. Reaction and cluster identification

The initialization procedure is performed for both projectile and target nuclei, which are then boosted against each other in their center-of-mass frame. We interrupt the evolution of the system after 100–150 fm/$c$; at this point we identify the prefragments, we calculate their excitation energies, and we input this information into a statistical decay code, which handles the de-excitation of the prefragments and the production of the final fragments. The exact switching time between the dynamical stage and the decay stage is not very important as long as it is chosen in the interval indicated [7].

The identification of prefragments is done by a simple chain cluster rule: Two nucleons are assumed to belong to the same cluster if their phase-space distance is small enough. The excitation energy of the prefragments is calculated by subtracting the ground-state energy (according to the liquid-drop formula) from the prefragment total energy.

### E. Limitations

Although the JQMD model has been used with great success in the past to reproduce numerous measurable aspects of nuclear reactions, it was not until recently [9,14] that a thorough benchmark of fragment yields in heavy-ion reactions was attempted. The first results are encouraging but, at the same time, they unveiled a fundamental ambiguity in the model.

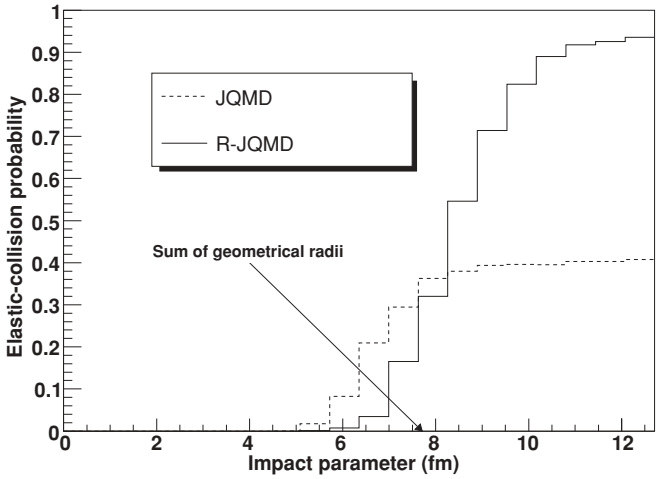


FIG. 1. Elastic-collision probability as a function of impact parameter for 1 $A$ GeV $^{40}$Ca + $^{40}$Ca.

We can illustrate this problem with Fig. 1, where the dashed line shows the probability of having an elastic collision as a function of the impact parameter, for a $^{40}$Ca + $^{40}$Ca reaction at 1 $A$ GeV, calculated with JQMD. A collision is judged to be elastic if no new particles are emitted (in either reaction step). (Here, the GEM code was used for the decay step.) Since the nuclear force has a very short range, we should expect that the probability for elastic collisions approach one as the impact parameter increases; however, Fig. 1 shows that this does not happen. Even at impact parameters much larger than the sum of the radii of the nuclei involved, inelastic collisions are still very likely. The nuclei considered here are also light enough that any other inelastic channel (such as electromagnetic dissociation) can safely be neglected.

This result (whose validity is not restricted to the system discussed here) demonstrates that most peripheral collisions are spuriously labeled as inelastic because of spontaneous emission of nucleons or other particles. There are two mechanisms that could be responsible for this: Either nucleons are spontaneously emitted during the dynamical step of the reaction or nuclei accumulate in the dynamical step some unphysical excitation energy that is released in the decay step by emission of nucleons or $\gamma$ rays.

Why do we see these fluctuations between potential and kinetic energy? One reason is that, even though the effective potential $\langle \hat{V} \rangle$ is defined to be a Lorentz scalar [owing to the prescription defined by Eq. (5)], the equations of motion [Eqs. (4)] are not Lorentz-covariant since the Hamiltonian [Eq. (3)] is written noncovariantly as the sum of kinetic energy and potential energy; the covariant version of Eq. (3) is

$$H = \sum_i \sqrt{\boldsymbol{p}_i{}^2 + m_i{}^2 + 2m_i V_i}, \tag{6}$$

where $V_i$ is the effective potential felt by the $i$th particle. Equation (6) also shows how particles pick up an effective mass $m_i^* \equiv \sqrt{m_i{}^2 + 2m_i V_i}$ as an effect of the interaction with the other particles. The noncovariance of the equations of motion of JQMD means that the dynamics will be different depending on the frame of reference; hence, when nuclei are boosted to

the reaction frame, spurious fluctuations can arise and cause emission of particles in the dynamical step or in the decay step.

It is possible to modify the equations of motion by substituting the covariant Hamiltonian Eq. (6) into Eq. (3); formal justification for this will be given in Sec. III. However, it is important to remark here that the equations of motion are not the only source of fluctuations; the initial condition also plays an important role. Recall (see Sec. II C) that the initial condition is not the classical ground state of the system, but a configuration optimized to reproduce some known properties of the quantum-mechanical ground state. How this configuration is realized in practice is at least as important as the equations of motion for the stability of the system. In fact, it is always possible that one of the particles is ejected while the remaining bind together more closely. Furthermore, we should always keep in mind that any QMD model is a semiclassical $n$-body theory and, as such, exhibits chaos: thus, even if we knew exactly how to produce "stable" initial conditions, the evolution of the system would soon drift away from the trajectory we planned because (at least) of numerical noise. For all these reasons, we anticipate here that the problem of the ground-state instability cannot be solved solely by the implementation of a relativistically covariant formalism; however, as we will discuss in the following section, it is possible and necessary to approach the problem empirically.

## III. DESCRIPTION OF THE R-JQMD CODE

The R-JQMD code is a relativistically covariant version of JQMD that includes an empirically improved initialization procedure for nuclei. A similar but simpler model is described in Ref. [15].

### A. Dynamics

#### 1. Equations of motion

Currie, Jordan, and Sudarshan proved in the beginning of the 1960s [16] that the only dynamical system on a $6N$-dimensional phase space that admits a covariant Hamiltonian description is a collection of $N$ noninteracting particles (the no-interaction theorem); thus, if one wants to construct a relativistically covariant Hamiltonian formalism for a system of $N$ interacting particles, one needs to introduce additional degrees of freedom.

A covariant Hamiltonian for the $N$-particle system can be expressed in terms of $8N$ variables, $4N$ positional coordinates $q_{i\mu}$, and $4N$ momentum coordinates $p_{i\mu}$, which satisfy the four-dimensional Poisson brackets:

$$[p_{i\mu}, q_{j\nu}] = g_{\mu\nu}\delta_{ij},$$
$$[q_{i\mu}, q_{j\nu}] = [p_{i\mu}, p_{j\nu}] = 0.$$

Since we want to describe physical trajectories as world lines in the $8N$-dimensional phase space $\Gamma(8N)$, we have to eliminate $2N-1$ extra degrees of freedom and define a global time parameter $t$. This can be achieved with the help of $2N$ constraints

$$\phi_i = 0 (i = 1, \ldots, 2N).$$

According to Dirac's formulation of the constrained Hamiltonian system [17,18], the "Hamiltonian" is constructed as a linear combination of $2N-1$ constraints

$$H_c = \sum_{i=1}^{2N-1} u_i \phi_i,$$

with unknown Lagrange multipliers $u_i(t)$. Note that the $2N$th constraint is a definition of the time parameter $t$.

Since the constraints must be fulfilled for all times, their time derivatives with respect to the global time parameter $t$ must be zero; thus, one obtains the relations

$$\frac{d\phi_i}{dt} = \frac{\partial \phi_i}{\partial t} + [H_c, \phi_i] \approx 0, \tag{7}$$

where the symbol $\approx$ indicates that the equality has to be satisfied on the physical phase space [i.e., the $6N$-dimensional hypersurface $\Gamma(6N)$ defined by the constraints]. Equation (7) is rewritten as

$$\sum_{j=1}^{2N-1} S_{ij} u_j \approx -\frac{\partial \phi_{2n}}{\partial t}\delta_{i,2N}$$

with

$$S_{ij} \equiv -[\phi_i, \phi_j] = -\sum_{k=1}^{N}\left(\frac{\partial \phi_i}{\partial p_k}\frac{\partial \phi_j}{\partial q_k} - \frac{\partial \phi_i}{\partial q_k}\frac{\partial \phi_j}{\partial p_k}\right). \tag{8}$$

Here we should observe that the matrix $S$ is not freely dependent on the momenta $p_i$ and positions $q_i$. It is defined along the physical trajectory of the particles and the Lagrange multipliers $u_i$ depend only on $t$, not on $p_i$ and $q_i$. The equation of motion are given by

$$\frac{dq_i}{dt} = \frac{\partial H_c}{\partial p_i} = \sum_{j}^{2N-1} u_j \frac{\partial \phi_j}{\partial p_i}, \tag{9a}$$

$$\frac{dp_i}{dt} = -\frac{\partial H_c}{\partial p_i} = -\sum_{j}^{2N-1} u_j \frac{\partial \phi_j}{\partial q_i}. \tag{9b}$$

Following Refs. [10,11], we choose the on-mass-shell condition as follows:

$$\phi_i \equiv p_i^2 - m_i^2 - 2m_i\tilde{V}_i \, (i = 1, \ldots, n), \tag{10}$$

where $m_i$ and $\tilde{V}_i$ are the mass and the quasipotential of the $i$th particle, respectively. The total energy is given by

$$E_T = \sum_i (p_{i0} - m_i) = \sum_i \left(\sqrt{\boldsymbol{p}_i^2 + m_i^2 + 2m_i\tilde{V}_i} - m_i\right);$$

in the nonrelativistic limit, this becomes

$$E_T \simeq \sum_i \left\{\frac{\boldsymbol{p}_i^2}{2m_i} + \tilde{V}_i\right\}.$$

By choosing the quasipotential under the condition $\sum_i \tilde{V}_i = V_{int}^{NR}$, we can get a relativistic formulation consistent to the nonrelativistic framework.

In the nonrelativistic framework the interaction potential depends on the square of the two-particle distance. In the relativistic framework we make this argument Lorentz-invariant

by operating the substitution

$$\boldsymbol{r}_{ij} \to \tilde{\boldsymbol{r}}_{ij} = -q_{Tij}^2 = -q_{ij}^2 + (q_{ij} \cdot p_{ij})/p_{ij^2}$$

with

$$q_{ij} = q_i - q_j, \quad p_{ij} = p_i + p_j.$$

The squared transverse four-distance $q_{Tij}^2$ is a Lorentz scalar and reduces to the usual squared distance $\boldsymbol{r}_{ij}^2$ in the center-of-mass frame of particles $i$ and $j$ [10,11]. This prescription gives the JQMD potential, which reads [7]

$$\begin{aligned} V = {} & \frac{A}{2\rho_0}\sum_i \langle\rho_i\rangle + \frac{B}{(1+\tau)\rho_0{}^\tau}\sum_i \langle\rho_i\rangle^\tau \\ & + \frac{1}{2}\sum_i\sum_{j\neq i} c_i c_j \frac{e^2}{|\tilde{\boldsymbol{r}}_{ij}|}\,\mathrm{erf}(|\tilde{\boldsymbol{r}}_{ij}|/\sqrt{4L}) \\ & + \frac{C_s}{2\rho_0}\sum_i\sum_{j\neq i}(1-2|c_i-c_j|)\langle\rho_{ij}\rangle, \end{aligned}$$

where

$$\begin{aligned} \langle\rho_i\rangle &= \sum_{j\neq i}\langle\rho_{ij}\rangle, \\ \langle\rho_{ij}\rangle &= (4\pi L)^{-3/2}\exp(-\tilde{\boldsymbol{r}}_{ij}^2/4L), \end{aligned}$$

the variable $c_i$ is one for protons and zero for neutrons, $e$ is the elementary charge, and erf is the error function (for the numerical values of the free parameters, see Ref. [7]). The one-particle potentials are thus defined as

$$\begin{aligned} \tilde{V}_i \equiv {} & \frac{A}{2\rho_0}\langle\rho_i\rangle + \frac{B}{(1+\tau)\rho_0{}^\tau}\langle\rho_i\rangle^\tau \\ & + \frac{1}{2}\sum_{j\neq i} c_i c_j \frac{e^2}{|\tilde{\boldsymbol{r}}_{ij}|}\,\mathrm{erf}(|\tilde{\boldsymbol{r}}_{ij}|/\sqrt{4L}) \\ & + \frac{C_s}{2\rho_0}\sum_{j\neq i}(1-2|c_i-c_j|)\langle\rho_{ij}\rangle. \end{aligned} \tag{11}$$

To obtain the equations of motion we need to introduce $N$ further constrains, called "time fixations," to determine the time coordinates $q_{0i}$. In the full relativistic QMD formulation [10,11], time fixations are chosen in a rather involved way and make it necessary to invert the $2N$-dimensional matrix $S_{ij}$ [Eq. (8)] at all time steps, consuming a great deal of CPU time.

In high-energy reactions, two-body collisions are dominant; the purpose of the Lorentz-covariant formalism is only to describe relatively low energy phenomena between particles in a fast-moving medium. Therefore, we assume a simpler form for the time fixations, namely we set the time coordinates of all the particles to be the same. Explicitly, we use the following constraints:

$$\phi_{i+N} \equiv a \cdot (q_i - q_N) \quad (i = 1, \ldots, N-1), \tag{12a}$$

$$\phi_{2N} \equiv a \cdot q_N - t. \tag{12b}$$

If we choose the four-vector $a$ as $(1;\mathbf{0})$ in the calculation frame, we explicitly break Lorentz covariance and all the time coordinates become equal to $t$ ($q_{0i} = t$). The zeroth components of the positional coordinates, $q_{0i}$, have the meaning of time only in the calculation frame.

In the Skyrme-type interaction [Eq. (11)], the mean field is much smaller than the mass plus the kinetic energy; that is,

$$\boldsymbol{p}_i^2 + m_i^2 \gg 2m_i\tilde{V}_i. \tag{13}$$

We can then take the energy coordinate $p_{0i}$ to be equal to mass plus kinetic energy in the argument of the quasipotential $\tilde{V}_i$. Under this approximation, the constrains satisfy

$$\begin{aligned} \frac{\partial\phi_i}{\partial p_{0j}} &= 2\delta_{ij}p_{0i}\ (i = 1, \ldots, N), \\ \frac{\partial\phi_{i+N}}{\partial q_j} &= 2a(\delta_{ij} - \delta_{jN})\ (i \neq N), \\ \frac{\partial\phi_{2N}}{\partial q_j} &= 2a\delta_{jN}. \end{aligned}$$

Then $S_{ij}$ given by

$$\begin{aligned} S_{i+N,j} &= 2\big(p_i^0 - p_N^0\big)\delta_{ij}(1-\delta_{iN}) + 2p_i^0\delta_{ij}\delta_{iN}, \\ S_{i+N,j+N} &= 0, \end{aligned}$$

and the Lagrange multipliers $u_i$ are the solutions of the following equations:

$$\sum_{j=1}^{N} S_{i+N,j}u_j = 2p_i^0u_i - 2p_N^0u_N = 0\ (i \neq N),$$

$$\sum_{j=1}^{N} S_{2N,j}u_j = 2p_N^0u_N = 1,$$

namely

$$u_i = \frac{1}{2p_i^0} = \frac{1}{\sqrt{\boldsymbol{p}_i^2 + m_i^2 + 2m_i\tilde{V}_i}}\ (i = 1, \ldots, N).$$

Substituting these $u_i$ into Eqs. (9), we get the equation of motions with respect to $\boldsymbol{r}_i$ and $\boldsymbol{p}_i$ as

$$\begin{aligned} \frac{d\boldsymbol{r}_i}{dt} &= \frac{\boldsymbol{p}_i}{2p_i^0} + \sum_j \frac{2m_j}{2p_j^0}\frac{\partial\tilde{V}_j}{\partial\boldsymbol{p}_i} \\ &= \frac{\partial}{\partial\boldsymbol{p}_i}\sum_j\sqrt{\boldsymbol{p}_j^2 + m_j^2 + 2m_j\tilde{V}}, \end{aligned} \tag{14a}$$

$$\begin{aligned} \frac{d\boldsymbol{p}_i}{dt} &= -\sum_j \frac{2m_j}{2p_j^0}\frac{\partial\tilde{V}_i}{\partial\boldsymbol{r}_i} \\ &= \frac{\partial}{\partial\boldsymbol{r}_i}\sum_j\sqrt{\boldsymbol{p}_j^2 + m_j^2 + 2m_j\tilde{V}}. \end{aligned} \tag{14b}$$

#### 2. *Cluster separability and world-line invariance*

Our new formalism satisfies the properties of *cluster separability* and *world-line invariance*. Cluster separability means that if the system splits into clusters whose four-distances are spacelike and tend to infinity, then the dynamics of each of the clusters must be independent of the others. The proof that constraints of the form of Eqs. (10) and (12) satisfy this natural requirement has been given by Balachandran *et al.* [19]; therefore, we only need to consider world-line invariance.

The physical phase space $\Gamma(6N)$ defined by our constraints Eqs. (10) and (12) is not Poincaré-invariant; however, it is possible to construct a natural representation of the Poincaré group in the physical phase space. Consider an element $G$ of the Lie algebra of the Poincaré group; in general, the subgroup of canonical transformations generated by $G$ breaks the constraints since

$$[G, \phi_i] \neq 0$$

for some $i$. Define the modified generator

$$G^* \equiv G - \sum_{r,s=1}^{2N} [G, \phi_r] C_{rs} \phi_s, \tag{15}$$

where $C = -S^{-1}$. It can be easily proven [10] that, for arbitrary $G$ and $\bar{G}$,

$$[G^*, \bar{G}^*] \approx [G, \bar{G}],$$

which means that the starred Lie algebra is isomorphic to the nonstarred one. Moreover,

$$[G^*, \phi_i] \approx 0 \quad \forall i.$$

Thus, the starred generators $G^*$ generate a canonical representation of the Poincaré group that respects the constraints; we will refer to transformations in this group as "starred" for simplicity.

Consider now the single-particle Minkowski subspace of the spatial coordinates of one of the particles that can be obtained by projection of the complete phase space $\Gamma(8N)$. In principle, we have two natural ways of defining Poincaré transformations on this space:

(i) Poincaré transformations are the projections of the orbits of the starred Poincaré group onto the Minkowski subspace of spatial coordinates.
(ii) Poincaré transformations are the affine transformations

$$q'^{\mu} \equiv \Lambda^{\mu}{}_{\nu} q^{\nu} + k^{\mu}.$$

The requirement of world-line invariance is that these two definitions should be compatible, in the following sense: Given a particle world line, application of the two definitions of Poincaré transformations must produce the same set of events. It is allowed that a given point $q$ is transformed into different points $q^*$ and $q^\dagger$, as long as $q^*$ and $q^\dagger$ belong to the same world line.

It is sufficient to show world-line invariance for infinitesimal transformations, and for simplicity of notation we assume that $G^*$ is an element of the Lorentz group (i.e., we do not consider translations). The infinitesimal canonical transformation generated by $G^*$ is

$$\left(\delta q_k^{\mu}\right)_{\text{canonical}} = \left[G^*, q_k^{\mu}\right] \delta\lambda,$$

where $\delta\lambda$ is a small parameter. The corresponding infinitesimal linear transformation is

$$\left(\delta q_k^{\mu}\right)_{\text{geometrical}} = \omega^{\mu}{}_{\nu} q_k^{\nu} \delta\lambda,$$

with $\omega_{\mu\nu} = -\omega_{\nu\mu}$.

World-line invariance amounts to requesting that $(\delta q_k^{\mu})_{\text{canonical}}$ and $(\delta q_k^{\mu})_{\text{geometrical}}$ belong to the same world line; that is,

$$\left(\delta q_k^{\mu}\right)_{\text{canonical}} - \left(\delta q_k^{\mu}\right)_{\text{geometrical}} = \left[H, q_k^{\mu}\right] f_k \delta\lambda, \tag{16}$$

for some phase-space function $f_k$. Using Eq. (15) and remembering that

$$\left[G, q_k^{\mu}\right] = \omega^{\mu}{}_{\nu} q_k^{\nu},$$

we can rewrite Eq. (16) as

$$\sum_{r,s=1}^{2N} [G, \phi_r] C_{rs} \left[\phi_s, q_k^{\mu}\right] \approx \left[H, q_k^{\mu}\right] f_k \quad (k = 1, \ldots, N). \tag{17}$$

This is the world-line invariance condition.

To show that R-JQMD satisfies Eq. (17), we observe that

$$C_{ij} = 0, \quad C_{i+N, j+N} \simeq 0 \quad (i, j = 1, \ldots, N);$$

Eq. (17) becomes

$$\sum_{r,s=1}^{N} [G, \phi_r] C_{r+N,s} \left[\phi_s, q_k^{\mu}\right] \approx \left[H, q_k^{\mu}\right] f_k \quad (k = 1, \ldots, N).$$

However, for $s = 1, \ldots, N$,

$$\begin{aligned}
\left[\phi_s, q_k^{\mu}\right] &= \delta_{sk} \left[\phi_k, q_k^{\mu}\right] = 2\delta_{sk} \left[\frac{\phi_k}{2p_{0,k}} p_{0,k}, q_k^{\mu}\right] \\
&= 2\delta_{sk} \left( p_{0,k} \left[\frac{\phi_k}{2p_{0,k}}, q_k^{\mu}\right] + \frac{\phi_k}{2p_{0,k}} \left[p_{0,k}, q_k^{\mu}\right] \right) \\
&= 2\delta_{sk} \left( p_{0,k} \left[H, q_k^{\mu}\right] + \frac{\phi_k}{2p_{0,k}} \delta_0^{\mu} \right) \\
&\approx 2\delta_{sk} p_{0,k} \left[H, q_k^{\mu}\right];
\end{aligned}$$

thus,

$$\begin{aligned}
&\sum_{r,s=1}^{N} [G, \phi_r] C_{r+N,s} \left[\phi_s, q_k^{\mu}\right] \\
&\quad \approx \left[H, q_k^{\mu}\right] \left( 2p_{0,k} \sum_{r=1}^{N} [G, \phi_r] C_{r+N,k} \right),
\end{aligned}$$

which is of the form of Eq. (17) and proves world-line invariance.

### 3. *Collisions*

The treatment of two-body collisions has been left substantially unaltered in R-JQMD: production and decay of $\Delta(1232)$ and $N^*(1440)$ resonances are included, as well as production and absorption of pions. The production of resonances of higher mass has not been included yet: Thus, neither JQMD nor R-JQMD can be applied to reactions with energy higher than 4–5 *A* GeV. Extension of the higher hadron-hadron collisional processes is now in progress by introducing the cross sections generated by the JAM code [20].

Although no new collision channel has been included in R-JQMD, relativistic covariance introduces one important difference about the way energy and momentum conservation

are ensured, which we will illustrate by discussing elastic nucleon-nucleon scattering (the idea being the same for all collisions). The angular distribution of the scattering process is assumed to be known and is computed according to Cugnon's parametrization [21–23]; a random angle is drawn from this distribution, so the only quantity that must be determined is the energy of the outgoing particles. In nonrelativistic JQMD, this is done easily by applying energy and momentum conservation. In relativistic JQMD, however, the $i$th particle has an effective mass

$$m_i^* = \sqrt{{m_i}^2 + 2m_i V_i} \tag{18}$$

that depends on the one-particle effective potential $V_i$ and, thus, on the momenta of all the particles. Since the collision changes the particle momenta, it will also change all the effective masses, which then must be determined iteratively and self-consistently:

(i) start with the assumption that the outgoing particles keep the same effective masses as before the collision;
(ii) use energy and momentum conservation to calculate the particle energies after the collision;
(iii) recalculate the effective potentials $V_i$ and effective masses [according to Eq. (18)] for all the particles;
(iv) recalculate the total energy of the system;
(v) if the fractional change in total energy is smaller than $10^{-4}$, exit the loop; otherwise, go to step 2.

This procedure guarantees energy conservation for the whole system, but at the same time it lengthens the time needed for the calculation. In any case, the increase is not dramatic (of the order of 10%–20%), since Eq. (13) ensures that more than a couple of iterations are seldom necessary for convergence.

### B. Initialization

As we have anticipated, the implementation of a relativistically covariant dynamics does not guarantee the stability of two boosted nuclei in a very peripheral collision over the desired time span. Since it is difficult to formulate an initialization recipe that ensures stability, we decided to take a very simple empirical approach.

The initial state of a nucleus is created in the same way as in JQMD (Sec. II C), but an additional criterion is imposed: The state is boosted in the reaction center-of-mass frame and is let to evolve according to Eqs. (14) for the time span of the reaction; the initial state is then accepted only if no nucleons were emitted and potential-energy fluctuations are smaller than the threshold for particle evaporation.

The new initialization criterion obviously slows down the initialization procedure. For heavy nuclei the impact can be quite large, because the integration of the equation of motion is more time consuming and because it is more difficult to create stable configurations. However, the additional criterion does not have to be applied always; if the collision is sufficiently central, chances are high that the collision would be inelastic anyway. It is important to use the new initialization criterion only for those impact parameters for which there is a non-negligible probability of elastic collision. This simplification speeds up the initialization procedure sensibly, since the probability distribution of impact parameters must anyway be cut at some maximum value: Thus, the additional criterion needs to be applied only to a small fraction of all reactions. Motivated by these considerations, we have chosen to apply the additional initialization criterion only if the impact parameter (in femtometers) is greater than $A_P^{1/3} + A_T^{1/3}$, where $A_P$ and $A_T$ are the mass numbers of projectile and target.

## IV. VALIDATION

We present in this section a comparison between the results of calculations performed with R-JQMD and with JQMD.

### A. Consistence of boosted wave packets

We begin by showing the relevance of a relativistic treatment of nucleon-nucleon interactions. First, we want to quantify the importance of the new equations of motion [Eqs. (14)] for the dynamics of fast heavy ions. Ideally, the time evolution of the system should be compatible with transformations of the Lorentz group, in the following sense: Given an initial condition, one must obtain the same final state by letting the system evolve and then performing a Lorentz transformation, or by performing the Lorentz transformation first and then letting the system evolve.

The degree to which this is realized in JQMD/R-JQMD can be expressed quantitatively in the following way: Let $\boldsymbol{r}_i(t)$ and $\boldsymbol{p}_i(t)$ represent the trajectories of a system of nucleons with respect to a center-of-mass observer and let $\boldsymbol{r}'_i(t')$ and $\boldsymbol{p}'_i(t')$ represent the same trajectories with respect to a boosted observer. Note that we have to satisfy the requirement of equal time for all particles, Eqs. (15); thus, we use the following boost [24]:

$$\begin{aligned} r_{x,i}(t) &= r'_{x,i}(t'), \quad r_{y,i}(t) = r'_{y,i}(t'), \\ r_{z,i}(t) &= \gamma[r'_{z,i}(t') - \beta t'], \end{aligned} \tag{19a}$$

$$\begin{aligned} p_{x,i}(t) &= p'_{x,i}(t'), \quad p_{y,i}(t) = p'_{y,i}(t'), \\ p_{z,i}(t) &= [p'_{z,i}(t') - P_z]/\gamma, \end{aligned} \tag{19b}$$

$$t' = \gamma t, \tag{19c}$$

where $\beta$ is the boost velocity in units of $c$, $\gamma$ is the corresponding Lorentz factor, and $P_z$ is the center-of-mass momentum of the system. Given an initial condition $[\boldsymbol{r}_i(0), \boldsymbol{p}_i(0)]$ in the center-of-mass system, we derive boosted initial conditions using Eqs. (19); then we integrate numerically the equations of motion for both cases. The boosted phase-space coordinates $[\boldsymbol{r}'(t), \boldsymbol{p}'(t)]$ can then be transformed back and compared with the evolution of the center-of-mass system.

The comparison is carried out quantitatively by calculating the phase-space overlap of center-of-mass and boosted wave packets. Let $|\varphi(\boldsymbol{r}_i, \boldsymbol{p}_i)\rangle_i$ represent the wave packet of the $i$th nucleon with position $\boldsymbol{r}_i$ and momentum $\boldsymbol{p}_i$, as described by Eq. (1). The overlap of two different states is given by

$$|\langle\varphi(\boldsymbol{r}', \boldsymbol{p}')|\varphi(\boldsymbol{r}, \boldsymbol{p})\rangle_i|^2 = \exp\left[-\frac{(\boldsymbol{r} - \boldsymbol{r}')^2}{4L} - \frac{L(\boldsymbol{p} - \boldsymbol{p}')^2}{\hbar^2}\right].$$

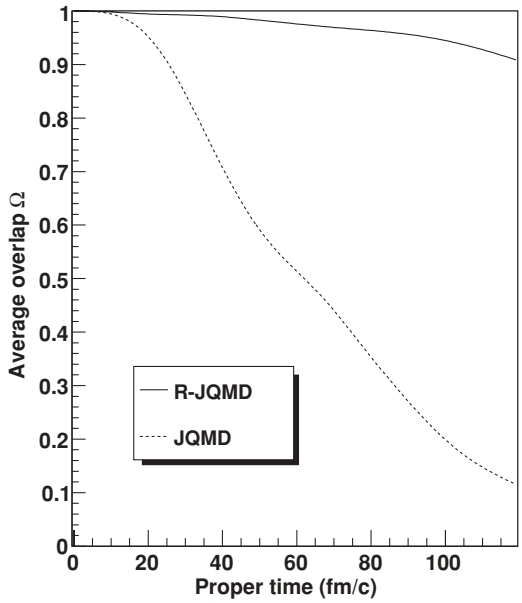


FIG. 2. Evolution of the average overlap [Eq. (20)] as a function of the proper time of a $^{40}$Ca nucleus boosted at $\gamma \simeq 1.24$.

The total wave function $|\psi\rangle$ is the direct product of the single-particle wave functions:

$$|\psi\rangle = \bigotimes_{i=1}^{A} |\varphi(\boldsymbol{r}_i, \boldsymbol{p}_i)\rangle_i .$$

Thus, we define the average overlap $\Omega$ as

$$\Omega \equiv |\langle\psi'|\psi\rangle|^{2/A} = \left(\prod_{i=1}^{A} |\langle\varphi(\boldsymbol{r}'_i, \boldsymbol{p}'_i)|\varphi(\boldsymbol{r}_i, \boldsymbol{p}_i)\rangle_i|^2\right)^{1/A}$$
$$= \exp\left[-\sum_{i=1}^{A}\left(\frac{(\boldsymbol{r}_i - \boldsymbol{r}'_i)^2}{4L} + \frac{L(\boldsymbol{p}_i - \boldsymbol{p}'_i)^2}{\hbar^2}\right)\Big/ A\right]. \quad (20)$$

Figure 2 shows the evolution of the average overlap of a $^{40}$Ca nucleus boosted at $\gamma \simeq 1.24$ as a function of the proper time of the nucleus; the value of the Lorentz factor corresponds to a $^{40}$Ca-$^{40}$Ca collision in the center-of-mass system, at 1 GeV/nucleon laboratory energy. The dynamics of heavy-ion collisions is typically followed for about 100 fm/$c$ in the collision center-of-mass system, which corresponds to (100 fm/$c$)/$\gamma \simeq 81$ fm/$c$ proper time. It is apparent that R-JQMD's equations of motion are much more stable than JQMD's over this time span.

### B. Directed transverse momentum

We turn now to the effect of the new equations of motion on measurable quantities. Not all observables in heavy-ion collisions are sensitive to relativistic corrections; Danielewicz and Odyniec [25] have identified transverse flow as a good candidate to emphasize the effect of a relativistic treatment. Therefore, as a measure of transverse flow, we show in Fig. 3 a plot of the time evolution of the directed transverse momentum $p^{\perp,\mathrm{dir}}$ for a $^{40}$Ca + $^{40}$Ca reaction at 1 $A$ GeV laboratory energy and impact parameter $b = 4.0$ fm. The directed transverse momentum is defined as

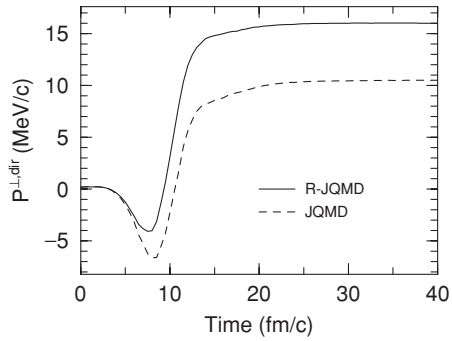


FIG. 3. Time evolution of the directed transverse momentum $p^{\perp,\mathrm{dir}}$ for a $^{40}$Ca + $^{40}$Ca reaction at 1 $A$ GeV laboratory energy and impact parameter $b = 4.0$ fm. The R-JQMD results are qualitatively consistent with the results of other relativistic QMD models [11,26].

$$p^{\perp,\mathrm{dir}} \equiv \sum_i p_i^{\perp}\ \mathrm{sign}\left(p_i^{\parallel}\right),$$

where the sum runs on all particles in the system, $p_i^{\parallel}$ represents the momentum component parallel to the beam axis *in the center-of-mass frame*, and $p_i^{\perp}$ is the momentum component perpendicular to the beam direction and lying in the reaction plane. Figure 3 demonstrates that R-JQMD predicts about 1.5 times larger directed transverse momentum than JQMD, in qualitative agreement with the results obtained by other relativistic QMD-like codes [11,26].

Observables other than those mentioned here are not as sensitive to relativistic effects; thus, one should not expect large differences in the results from R-JQMD and JQMD. We have verified this by computing double-differential energy-angle cross sections for production of neutrons in proton-nucleus collisions (Figs. 4 and 5). The JQMD results are taken from Ref. [7], and the experimental data are from Refs. [27] and [28]. It is clear that R-JQMD and JQMD do not differ very much as far as neutron spectra are concerned.

Finally, we checked the efficiency of the new ground-state initialization prescription by running nucleus-nucleus collisions at impact parameter equal to a few nuclear radii. We found that more than 90% of such collisions are judged as elastic by R-JQMD, which shows that the new initialization is quite effective. (See also Fig. 1, where the solid line depicts the elastic-collision probability for R-JQMD.) Spontaneous particle emission is almost never observed; the small, remaining fraction of spurious inelastic events is usually due to potential-energy fluctuations.

## V. HEAVY-ION FRAGMENTATION CROSS SECTIONS

In nuclear physics experiments, for example in measurement of heavy-ion fragmentation, the impact parameter of the

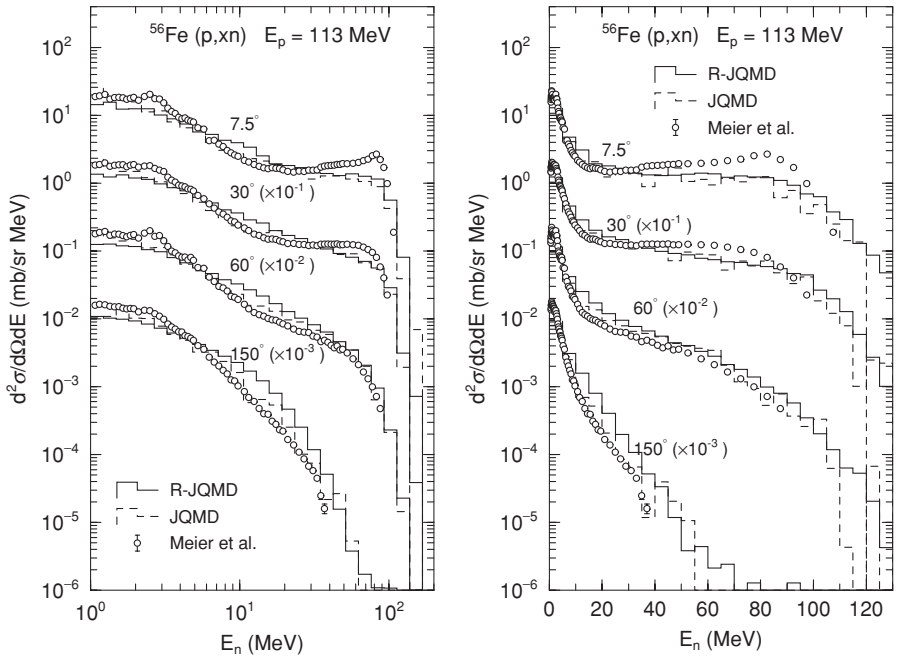


FIG. 4. Double-differential energy-angle cross sections for the production of neutrons in the reaction between 113-MeV protons and iron, with data taken from Ref. [27], on a log scale (left) and on a linear scale (right). No significant difference can be observed between JQMD and R-JQMD.

reaction remains always unobserved.[1] Thus, it is only possible to measure impact-parameter-integrated quantities, such as fragmentation cross sections, which can subsequently be used to validate nuclear-reaction and statistical-decay models such as JQMD/R-JQMD. To do this, it is necessary to impose a cutoff value for the impact parameter in the calculation, above which no collision is considered. The distribution of impact parameters below the cutoff value $b_{\max}$ is usually taken to be triangular; that is, the probability $p(b)\mathrm{d}b$ of collisions with impact parameter between $b$ and $b + \mathrm{d}b$ is given by

$$f(b) = \begin{cases} 2b/b_{\max}^2 & \text{if} \quad b \leqslant b_{\max}, \\ 0 & \text{if} \quad b > b_{\max}. \end{cases} \tag{21}$$

However, if ground-state instabilities affect fragmentation yields in peripheral collisions (as happens in JQMD), different choices of $b_{\max}$ will produce different fragmentation cross sections. The effect can be sizable; in previous JQMD calculations [9,29], in fact, the $b_{\max}$ value had been fixed to fit measured total charge-changing cross sections. Ideally, nonetheless, one would like to keep the number of free parameters in the code to a minimum and eliminate the

[1] It is nevertheless possible to operate a gross discrimination between central and peripheral collisions by looking, for example, at the reaction multiplicity.

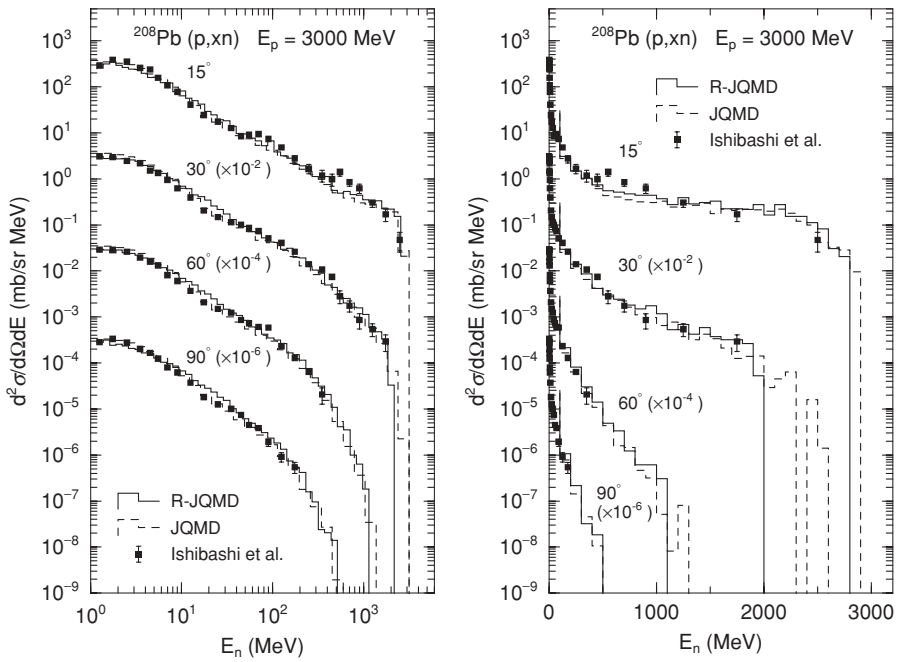


FIG. 5. Double-differential energy-angle cross sections for the production of neutrons in the reaction between 3-GeV protons and lead, with data taken from Ref. [28], on a log scale (left) and on a linear scale (right). No significant difference can be observed between JQMD and R-JQMD.

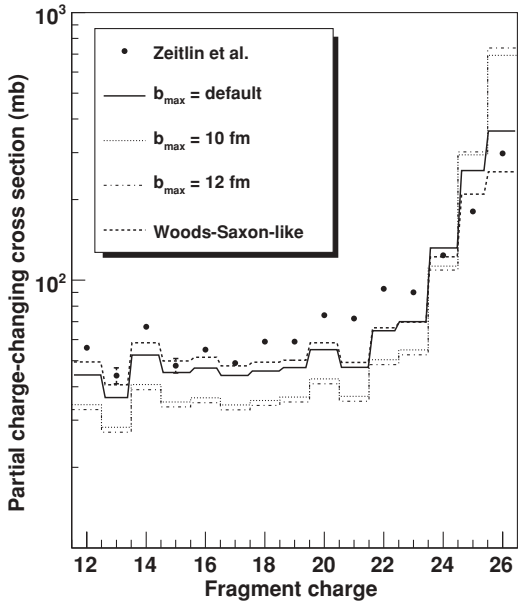


FIG. 6. Fragmentation cross sections for 1 $A$ GeV $^{56}$Fe on Al, calculated with different impact-parameter distributions. Experimental data are taken from Ref. [30].

dependency of the fragmentation cross sections on the value of $b_{\max}$.

It would seem that this program is now feasible with R-JQMD. As long as $b_{\max}$ is larger than a certain threshold, in fact, the cross sections will exhibit little sensitivity to the exact cutoff; for example, for 1 $A$ GeV $^{40}$Ca + $^{40}$Ca this threshold lies around 11 fm, as Fig. 1 suggests. Unfortunately, "asymptotic" cross sections (i.e., those calculated with a very large impact parameter value) agree very poorly with the measurements, as Fig. 6 shows. The cross sections for heavy fragments are largely overestimated and the cross sections for lighter fragments are underestimated (but the reaction cross section is kept constant); that is, too many peripheral collisions occur. This is probably caused by the large width of wave packets (see Sec. II A): The nucleon wave packets, in fact, have a fixed width $L = 2$ fm$^2$ that is responsible for a wide nuclear skin thickness that enhances very soft, peripheral reactions.

### A. Optimization of the impact-parameter distribution

This negative result indicates that very accurate prediction of heavy-ion fragmentation cross sections is beyond the capabilities of JQMD/R-JQMD (but the accuracy that one can achieve is nonetheless sufficient for several applications; see, e.g., Ref. [9]). Some semiempirical tuning parameter (such as $b_{\max}$) must be introduced if one wants to improve the agreement with the experimental data.

One idea is the following. Since the peripheral-collision yields in JQMD are distorted by the very broad nuclear surface thickness, one could try to suppress peripheral collisions by modifying the impact-parameter distribution. However, optimizing the impact-parameter distribution can be very time consuming if one intends to run a different calculation for each set of parameters in each impact-parameter distribution. This is not necessary, as we will illustrate in the following.

We need to make a clarification first. In principle, all QMD models are also able to calculate reaction cross sections for nucleus-nucleus reactions; in practice, however, the accuracy of the result is seldom sufficient for certain applications, notably radioprotection. Radiation-transport codes thus rely on separate models to calculate reaction cross sections and decide when (and where) a reaction should take place (see Ref. [31] for example); when this happens, collision events are repeated in the nuclear-reaction model (i.e., JQMD/R-JQMD) until an inelastic process occurs. This method has an important consequence; namely, the effective distribution of inelastic collisions, as a function of the impact parameter, will not be the same as the assumed distribution. For example, let us assume that we sample an impact parameter from the distribution of Eq. (21) and we run a collision; if the latter proves to be elastic, we have to resample the impact parameter and rerun the collision, according to what we have just described. But this means that the effective fraction of collisions with impact parameter $[b, b + \mathrm{d}b]$ will not be simply proportional to $f(b)$, but rather to the product $f(b)p_{\mathrm{inel}}(b)$, where $p_{\mathrm{inel}}(b)$ is the probability of having an inelastic collision at impact parameter $b$.

Now we can turn to our method to optimize impact-parameter distributions. It is actually sufficient to run only one calculation for each projectile-target combination and to calculate the probability $p_Z(b)$ that a collision at impact parameter $b$ produces a leading fragment with charge $Z$; the sum $\sum_Z p_Z(b)$ is actually nothing but the inelastic-collision probability $p_{\mathrm{inel}}(b)$ previously defined. By knowing these quantities and the reaction cross section $\sigma_{\mathrm{reaction}}$, it is possible to calculate fragmentation cross sections for any impact-parameter distribution $f(b)$. One considers the effective distribution

$$f_{\mathrm{eff}}(b) \equiv f(b)p_{\mathrm{inel}}(b) \Big/ \int_0^\infty f(b)p_{\mathrm{inel}}(b)\,\mathrm{d}b;$$

the probability of producing a fragment with charge $Z$ is then

$$p_Z = \int_0^\infty f_{\mathrm{eff}}(b)p_Z(b)\,\mathrm{d}b,$$

and the fragmentation cross section is simply

$$\sigma_Z = \sigma_{\mathrm{reaction}}\,p_Z.$$

Therefore, our method allows us to calculate fragmentation cross sections for any impact-parameter distribution by running only one calculation.

As a test, we have modified Eq. (21) and introduced a Woods-Saxon-like shape, as follows:

$$f(b) = N\frac{b}{1 + \exp[(b - c_1)/c_2]}; \tag{22}$$

here $N$ is a normalization factor and $c_1$ and $c_2$ are two adjustable parameters. In the limit $c_2 \to 0$, Eq. (22) tends to Eq. (21), if one identifies $c_1$ with $b_{\max}$; for generic values of $c_2$, however, Eq. (22) describes a distribution that has a tail extending beyond $c_1$ and that favors central collisions with respect to Eq. (21). We optimized the parameters $c_1$ and $c_2$ by

minimizing a $\chi^2$ merit function. The resulting fragmentation cross sections (for the 1$A$ GeV $^{56}$Fe + Al system) are plotted in Fig. 6; the optimal parameter values are $c_1 = (6.98 \pm 0.02)$ fm and $c_2 = (0.35 \pm 0.03)$ fm (to be compared with the default $b_{\max} = 7.45$ fm). The Woods-Saxon-like cross sections agree better with the experimental data than the default triangular distribution, but the improvement is not dramatic; in other words, the fragmentation cross sections are quite stable with respect to the impact-parameter distribution. This conclusion has been confirmed by the analysis of other projectile-target combinations.

One can therefore conclude that no significant breakthrough in the accuracy of fragmentation cross sections can be achieved by tuning the impact-parameter distribution. It is possible that other distribution shapes give better agreement than the default triangular distribution or than the Woods-Saxon-like distribution, but, overall, cross sections appear to be quite insensitive to the detailed shape of the assumed impact-parameter distribution.

## VI. CONCLUSIONS

We have described the R-JQMD model, a relativistically covariant version of JQMD that features an improved ground-state initialization algorithm. We have outlined the main differences between the two models and we have compared the predictions of the new model with some experimental data.

We have shown that the R-JQMD model produces reasonably stable nuclei even in boosted frames of reference; even though the formalism is not explicitly covariant, we have seen that boosted and nonboosted equations of motion evolve with a much higher degree of coherence than in the old JQMD model. In view of these results, we claim that the R-JQMD model represents an excellent compromise between physical accuracy and calculation speed: it can produce accurate predictions of heavy-ion collisions at relativistic energies without calling for the full relativistic QMD machinery.

We have also investigated how easy it would be to improve heavy-ion fragmentation cross sections by tuning the impact-parameter distribution of collisions. The results are negative: on the one hand, JQMD/R-JQMD's broad nuclear surface thickness leads to overestimation of heavy-fragment yields and prevents the use of large cutoffs for the impact-parameter distribution; on the other hand, changing the shape of the impact-parameter distribution to enhance central collisions does not modify the cross sections dramatically.

## ACKNOWLEDGMENT

The authors would like to thank the referee for comments that improved the quality of the paper.

[1] H. Stöcker and W. Greiner, Phys. Rep. **137**, 277 (1986).
[2] J. Aichelin, Phys. Rep. **202**, 233 (1991).
[3] R. W. Minich *et al.*, Phys. Lett. **B118**, 458 (1982).
[4] J. Pochodzalla, Prog. Part. Nucl. Phys. **39**, 443 (1997).
[5] J. A. Simpson, Annu. Rev. Nucl. Part. Sci. **33**, 323 (1983).
[6] M. Durante, Riv. Nuovo Cimento **25**, 8 (2002).
[7] K. Niita, S. Chiba, T. Maruyama, T. Maruyama, H. Takada, T. Fukahori, Y. Nakahara, and A. Iwamoto, Phys. Rev. C **52**, 2620 (1995).
[8] S. Furihata, Nucl. Instrum. Methods B **171**, 251 (2000).
[9] L. Sihver, D. Mancusi, T. Sato, K. Niita, H. Iwase, Y. Iwamoto, N. Matsuda, H. Nakashima, and Y. Sakamoto, Adv. Space Res. **40**, 1320 (2007).
[10] H. Sorge, H. Stöcker, and W. Greiner, Ann. Phys. (NY) **192**, 266 (1989).
[11] T. Maruyama, S. W. Huang, N. Ohtsuka, G. Li, A. Fässler, and J. Aichelin, Nucl. Phys. **A534**, 720 (1991).
[12] S. R. Souza, L. de Paula, S. Leray, J. Nemeth, C. Ngô, and H. Ngô, Nucl. Phys. **A571**, 159 (1994).
[13] A. Bohr and B. R. Mottelson, *Nuclear Structure*, Vol. 1 (Benjamin, New York, 1969–1975), re-edited version (World Scientific, Singapore, 1998).
[14] D. Mancusi *et al.*, Nucl. Instrum. Methods B **254**, 30 (2007).
[15] T. Maruyama, K. Niita, T. Maruyama, S. Chiba, Y. Nakahara, and A. Iwamoto, Progr. Theor. Phys. **96**, 263 (1996).
[16] D. G. Currie, T. F. Jordan, and E. C. G. Sudarshan, Rev. Mod. Phys. **35**, 350 (1963).
[17] P. A. M. Dirac, Rev. Mod. Phys. **21**, 392 (1949).
[18] P. A. M. Dirac, Proc. R. Soc. London Ser. A **246**, 326 (1958).
[19] A. P. Balachandran, D. Dominici, G. Marmo, N. Mukunda, J. Nilsson, J. Samuel, E. C. G. Sudarshan, and F. Zaccaria, Phys. Rev. D **26**, 3492 (1982).
[20] Y. Nara, N. Otuka, A. Ohnishi, K. Niita, and S. Chiba, Phys. Rev. C **61**, 024901 (1999).
[21] G. F. Bertsch and S. Das Gupta, Phys. Rep. **160**, 189 (1988).
[22] J. Cugnon, T. Mizutani, and J. Vandermeulen, Nucl. Phys. **A352**, 505 (1981).
[23] J. Cugnon, Phys. Rev. C **22**, 1885 (1980).
[24] T. Maruyama, T. Maruyama, and K. Niita, Phys. Lett. **B358**, 34 (1995).
[25] P. Danielewicz and G. Odyniec, Phys. Lett. **B157**, 146 (1985).
[26] E. Lehmann, R. K. Puri, A. Faessler, G. Batko, and S. W. Huang, Phys. Rev. C **51**, 2113 (1995).
[27] M. M. Meier, D. A. Clark, C. A. Goulding, J. B. McClelland, G. L. Morgan, and C. E. Moss, Nucl. Sci. Eng. **102**, 310 (1989).
[28] K. Ishibashi *et al.*, J. Nucl. Sci. Technol. **34**, 529 (1997).
[29] T. Sato, L. Sihver, H. Iwase, H. Nakashima, and K. Niita, Adv. Space Res. **35**, 208 (2006).
[30] C. Zeitlin, L. Heilbronn, J. Miller, S. E. Rademacher, T. Borak, T. R. Carter, K. A. Frankel, W. Schimmerling, and C. E. Stronach, Phys. Rev. C **56**, 388 (1997).
[31] H. Iwase, K. Niita, and T. Nakamura, J. Nucl. Sci. Technol. **39**, 1142 (2002).